Escola de Primavera de Transição e Turbulência
Blumenau 2020

ABCM Associação Brasileira de Engenharia e Ciências Mecânicas

12th Spring School on Transition and Turbulence
September 21st-25th, 2020, Blumenau, SC, Brazil

# EPTT2020-0002
# INFLUENCE OF DOUBLE FLAME SPRAY PYROLYSIS ON NANOPARTICLE SIZE

**Nadine Zandoná Rafagnim**
**Pedro Bianchi Neto**
**Dirceu Noriler**
University of Campinas, Campinas, Brazil
dnoriler@unicamp.br

**Udo Fritsching**
Leibniz Institute for Materials Engineering IWT, Bremen, Germany
ufri@iwt.uni-bremen.de

***Abstract.*** *The ability to control particle size and distributions is a desired attribute of a nanoparticle production process. Among such processes, the Flame Spray Pyrolysis (FSP) can turn many elements of the periodic table into metal nanoparticles by the injection of a low-cost metallic precursor dissolved in a liquid fuel through a nozzle. A further step to FSP is the production of multicomponent nanoparticles in a double flame device (DFSP) where particle properties can be controlled through geometrical modifications. Many experimental works have compared nanoparticles produced by FSP and DFSP, focusing on specific desired properties. In this work, we aim to compare the techniques by analyzing agglomerates and primary particles sizes as well as thermal and chemical profiles. Therefore, Computational Fluid Dynamics was applied. The continuous gas phase is described by the Eulerian framework whilst a Lagrangian tracking is applied for the liquid phase. A monodisperse population balance model (PBM) describes the solid nanoparticles. Identical precursors and flow rates were considered for both nozzles in the double flame cases. The two-nozzle configuration influence is accessed by varying the intersection distance between flames. The main results emphasize the DFSP advantages over FSP on the particle size control, since the flame configuration has great influence on it. Furthermore, it was shown that the application of CFD coupled with a PBM on the description of nanoparticles is a viable technique.*

***Keywords:*** *Nanoparticles, Flame, Pyrolisis, Population Balance, CFD*

## 1. INTRODUCTION

An important position has been taken by nanostructures in the contemporary reality of production, optimization, development and application of materials. High surface area to volume ratio, chemical stability, catalytic properties, and thermal-mechanical resistance are some characteristics of nanoparticles of metallic oxides that have been drawing attention of the scientific community. These materials have applications that vary from fuel cells to paints, and from pharmacological products to pesticides (Mehta *et al.*, 2013; Wegner and Pratsinis, 2005). Heterogeneous catalysis is another example of application, in which multicomponent nanostructures, commonly made of supported noble metal oxides, are applied. Independently of the application, nanoparticle size directly influences the processes performance. Therefore, a recurrent challenge faced during the production of nanomaterials is the high dependence between operation conditions and the final characteristics of the product (Grossmann *et al.*, 2015). Conventional production processes, such as wet precipitation (Li *et al.*, 2006), precipitation deposition (Bamwenda *et al.*, 1997), and flame spray pyrolisis (FPS) (Mädler *et al.*, 2002), allow for the control of particle size through parameters such as residence time, temperature, pH, and flow rates. Among these methods, the FSP is particularly interesting for the synthesis of particles metallic oxides, given its high efficiency, low waste generation, and low energetic demand, when compared to other techniques. Such process allows for the efficient and economical production of materials with high purity and in a narrow range of sizes, from 1 to 200 nm.

In the FSP, the nanoparticles are obtained through the evaporation and the combustion of a spray of a mixture of fuels (ethanol, iso-octanes, aromatic hydrocarbons) and precursors (organometallics). The tiny droplets of the spray containing the dissolved precursor are dispersed with a jet of oxidant (air or pure oxygen), evaporate and burn, forming a turbulent flame. The main flame is stabilized with a pilot flame produced via the combustion of premixed gaseous hydrocarbons. The nanoparticles nucleate in the central region of the main flame, after evaporation and combustion of the precursor. Air of entrainment is responsible for the quenching of the system, and guarantees the supply of oxygen for complete

combustion of the fuels. Some of the advantages of this method include: the possibility of dissolving the precursor directly into the fuel used for the main flame, allowing for a simple introduction of the precursor into the reaction zone; the relatively easy collection of the final material downstream from the flame (usually with filters), without the need of further purification; the flexibility referent to material production, which allows for the use of virtually any element in the periodic table, via relatively cheap precursors (Mädler *et al.*, 2002; Teoh *et al.*, 2010).

For the production of multicomponent nanoparticles, the FSP can be adapted to include more than one metal in the fuel-precursor mixture, as shown by Strobel *et al.* (2006) for the production of $Pt/Al_2O_3$, and by Teoh *et al.* (2010), for $Pt/TiO_2$. The increase in precursor concentration, however, may generate undesirable larger agglomerates, due to higher concentration of particles in the lower regions of the reactor. A double flame configuration (DFSP) offers the possibility of individual formation of each component for a subsequent mixture, in a desirable regime. This allows for a finer control over multicomponent particle characteristics, making possible the production of material in a large range of compositions. Figure 1 shows the principles of agglomerate formation with the use of such technique for the production of nanoparticles. In the case of the DFSP, the intersection point between the flames, defined by the predetermined distance and angle of the nozzles, have direct influence over the final product morphology and composition. The intersection of the flames coinciding with the evaporation and nucleation zones may result in atomic bounds of the components, whereas larger distances between the flames favor the mixture of previously formed solid particles (Minnermann *et al.*, 2013). It is important to mention that asymmetric configurations, i.e. when the burners are not vertically aligned or do not present the same tilting angles, are also possible. These configurations make a vast variety of flame interactions available, but these will not be studied in this work.

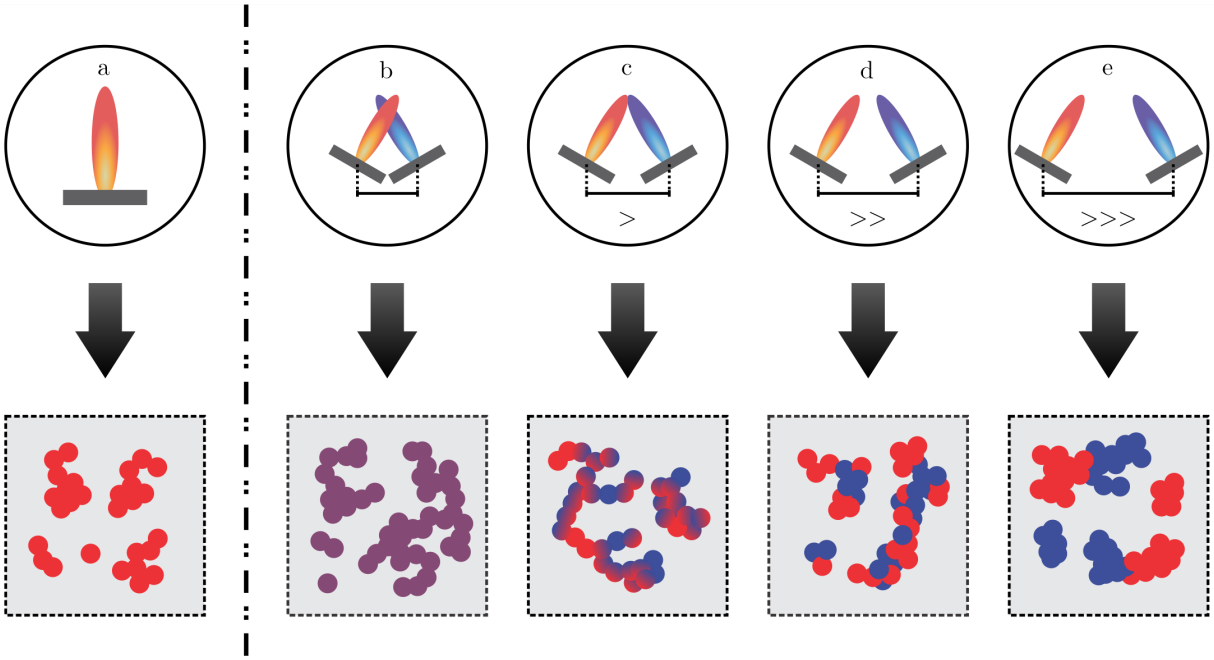


Figure 1. Basic morphology of agglomerates produced by FSP (a) and DFSP (b-e). From left to right, the distance between the flames (b-e) is increased.

The adaption of the FSP process for the manufacture of functional nanostructured materials, as well as its scale-up, requires the development of tools that integrate mathematical modeling and computational simulations. Such tools would make it possible to predict the main phenomena involved in the process, including the chemistry-turbulence interaction, the formation and evolution of the spray, mass and heat transfer, particle formation and growth, among others. The use of computational simulations, based on validated mathematical models, is valuable for reactor and process design. Modeling these phenomena, however, is a complex task and requires a deep understanding of the process. An example can be seen in the prediction of thermal and chemical profiles, that strongly influence particle nucleation and growth. Non-premixed turbulent flames, formed from atomized fuels, are typical for the FSP, and demand detailed models in order to produce realistic fields of temperature and chemical concentration. Some studies have been focused in the analysis of this step of the process (Noriler *et al.*, 2014a; Meierhofer *et al.*, 2014; Grossmann *et al.*, 2015), investigating the influence of the liquid spray over the main flame and other characteristics of the process.

Computational Fluid Dynamics (CFD) has shown good results as a tool for the study of the FSP process, especially when combined with Population Balance Models (PBM), that can describe the formation and evolution of the solid nanoparticles in relation to flame (Torabmostaedi *et al.* (2013); Gröhn *et al.* (2014); Torabmostaedi and Zhang (2014); Buss *et al.* (2018); Bianchi Neto *et al.* (2020); Buss *et al.* (2020)). Publications intending to advance in the understanding

of the phenomena involved in the DFSP, however, are mainly focused in experimental analyses, and with qualitative discussion of the results. Works with the use of CFD and with quantitative analyses are rare, e.g. Grossmann *et al.* (2015).

Population Balance Models (PBM) are intended for the prediction of the behavior of a population (of particles, in this case) in reference to the environment. For that, the population is described through the density of an adequate extensive variable, usually number of particles, mass or volume, depending on the system characteristics. Regular transport equations are then used to describe the behavior of these variables (Ramkrishna, 2000). An important aspect of the FSP is the fact that particles are being constantly created and evolving, due to the processes nucleation, agglomeration and sintering. The particles are represented by the PBM in two coordinate systems, the internal and the external. The former corresponds to quantitative characteristics that are used to describe the population (the extensive variable mentioned above), whereas the latter corresponds to the position of the population individuals in the physical space. In that sense, the particles can be described by the assemble of their internal and external coordinates, their so-called state space, that are useful for the prediction of systems such as the FSP.

In this study, we applied CFD techniques to simulate nanoparticle production via the FSP process, both single- and double-flamed. We used a monodisperse PBM, i.e. only in terms of mean values, to compare the resultant product from these different reactor configurations, and analyzed how the presence of a second flame (at two different distances between nozzles) influences the characteristics of the nanoparticles.

## 2. METHODOLOGY

In this paper, symmetric DFSP reactors are investigated. Two geometrical parameters are important to define the mixing region of the jets in these reactors: the angle between the nozzle centerline and vertical axis ($\alpha$) and the distance between the nozzle outlet and the point where the flame axis intersect (intersectional distance, I). In this paper, simulations for DFSP were carried out for flame settings of I = 100 and 200 mm, both for $\alpha$ = 20°, and compared with a single flame (FSP) case.

For all simulated cases, a 20% zirconium IV-propoxide ($C_{12}H_{28}O_4Zr$), 8% n-propanol ($C_3H_7OH$) and 72% ethanol ($C_2H_5OH$) solvent-precursor liquid mixture is injected at a flow rate of 5 mL/min through a conical surface above the nozzle. The droplets are dispersed by pure $O_2$ (5 L/min) fed at a constant pressure drop of 1.5 bar at the nozzle tip. The spray flames were ignited and stabilized with a premixed support flame of $CH_4$ (1.5 L/min) and $O_2$ (3.2 L/min) (Bianchi Neto *et al.*, 2020).

Following Noriler *et al.* (2014a), a steady-state two-phase Euler-Lagrange model was chosen to describe the continuous gas phase (Table 1) and the discrete liquid droplets (Table 2), respectively.

Table 1. Gas phase Eulerian governing equations

| Gas phase (Eulerian equations) | |
|---|---|
| • Continuity equation $\frac{\partial \rho}{\partial t} + \nabla \cdot (\rho \mathbf{v}) = \sum a_d M_d$ | (1) |
| • Momentum conservation equation $\frac{\partial}{\partial t}(\rho \mathbf{v}) + \nabla \cdot (\rho \mathbf{v}\mathbf{v}) = -\nabla p + \nabla \cdot \tau_{eff} + \rho \mathbf{g} - \sum \rho_d F_D (\mathbf{v} - \mathbf{u})$ | (2) |
| • Energy conservation equation $\frac{\partial}{\partial t}(\rho h) + \nabla \cdot (\rho \mathbf{v} h) = \nabla \cdot (\lambda_{eff} \nabla T) - \sum a_d \left[h_\infty (T - T_d) + h_{vap} M_d\right] - \nabla \cdot \mathbf{q}r - \sum_{r=1}^{rxn} h_{r,rx} R_r$ | (3) |
| • Chemical species conservation equation $\frac{\partial}{\partial t}(\rho Y_i) + \nabla \cdot (\rho \mathbf{v} Y_i) = -\nabla \cdot \mathbf{J}_{i,eff} + \sum Md, i \sum_{r=1}^{rxn} R_{i,r}$ | (4) |

Turbulence was described with the $k$-$\omega$ SST model, because it blends the $k$-$\omega$ near wall treatment with the free-steam $k$-$\epsilon$ models. A two-way coupling with turbulent dispersion between the gas and liquid phases was considered. The mass and heat interphase transfers of the vaporizing droplets were accounted by the Ranz and Marshall (1952) correlation to the Sherwood and Nusselt numbers. Radiation was described by the simple P-1 model, considering a grey gas model. For the reactive flow, fuel and solvent oxidation reactions were considered. A four-step mechanism was applied for methane combustion, whereas a single step mechanisms was employed for the remaining fuels. The Eddy Dissipation Concept (EDC) model was used to describe the interaction between turbulence and chemistry, assuming that the reactions occur

Table 2. Liquid phase Lagrangian governing equations

| Liquid phase (Lagrangian Equations) | |
|---|---|
| • Force balance for a droplet | |
| $m_d \frac{d\mathbf{u}}{dt} = m_d F_D(\mathbf{v}-\mathbf{u}) + m_d\left(\frac{\rho_d-\rho}{\rho_d}\right)\mathbf{g} - \mathbf{u}\frac{dm_d}{dt}$ | (5) |
| • Energy equation | |
| $\frac{m_d c_p}{A_d}\frac{dT_d}{dt} = h_\infty(T-T_d) + \epsilon_d\sigma\left(\theta_R^4 - T_d^4\right) + h_{vap}M_d$ | (6) |

in the fine scale turbulent structures, where the reactants are homogeneously mixed (Bianchi Neto *et al.*, 2018). For the single flame nozzle setup, a two-dimensional axissymmetrical approach was adopted (Noriler *et al.*, 2014b). For DFSP, however, a three dimensional domain was necessary due to the lack of axissymmetry of the reactor. The solution was carried out using the commercial code Fluent 14, from ANSYS.

For the solid phase, a monodisperse Population Balance Model (PBM), adapted from Bianchi Neto *et al.* (2018), was used to describe particle formation and mixture (Table 3). This PBM accounts for variations in number, area and volume concentrations of particle agglomerates which undergo nucleation, agglomeration and sintering.

Table 3. Solid phase Population Balance Model equations

| Solid Phase (Population Balance Equations) | |
|---|---|
| • Number concentration equation | |
| $\nabla\cdot(\rho\mathbf{v}N) - \nabla\cdot(\Gamma_t\nabla N) = k_f - \frac{1}{2}\beta(\rho N)^2$ | (7) |
| • Agglomerate surface area | |
| $\nabla\cdot(\rho\mathbf{v}A) - \nabla\cdot(\Gamma_t\nabla A) = k_f a_0 - \frac{\rho(A-Na_s)}{\tau_s}$ | (8) |
| • Agglomerate volume | |
| $\nabla\cdot(\rho\mathbf{v}V) - \nabla(\Gamma_t\nabla A) = k_f \mathrm{v}_0$ | (9) |

To estimate the discretization error, the Grid Convergence Index (GCI) of the axial temperature was evaluated for all geometries following the methodology proposed by Celik *et al.* (2008). Therefore, the results of three meshes with different refinement levels were compared. The computational time is significantly increased for the 3D geometries. For the I = 100 mm case, for instance, it takes about 95, 155 and 680 hours to simulate the flame with the course, medium and fine meshes, respectively, in a 28 cores Intel Xeon E5-2680 2.4 GHz of 132 GB RAM memory. Therefore, the results presented in this paper for the DFSP reactors were obtained with the medium mesh, whilst the FSP results are for the finer grid. The GCI results are presented in Table 4 with their respective mesh size for the (fine) 2D FSP case and (medium) 3D DFSP cases.

Table 4. Mesh characteristics: type, size, and grid convergence index (GCI).

| Cases | | Domain type | Mesh size (elements) | GCI[(1)] |
|---|---|---|---|---|
| FSP | | 2D-axissymetric | 243,325 | < 1.00% |
| DSFP | I = 100 mm | 3D | 2,576,142 | < 3.05% |
| | I = 200 mm | 3D | 3,588,380 | < 2.15% |

(1) values calculated based on temperature profiles.

## 3. RESULTS AND DISCUSSION

In this section, obtained results for all considered cases are compared and discussed. The discussion is segmented into two parts. The first regards the flame spray, and its main characteristics. The second, the produced nanoparticles.

### 3.1 Flame Spray

The flame profiles are crucial for the application of the PBM in these simulations, especially given the one-way coupling method adopted (between solid and gas phases). In this sense, firstly, flame profiles such as of velocity and temperature, will be compared.

#### 3.1.1 Air Entrainment

Figure 2 shows the obtained contours of velocity for each considered case. As it is shown, similar profiles were achieved, what is expected given the similar conditions adopted, regarding flow-rates. Supersonic velocities are observed right at the nozzle exit, what provides energy for spray atomization. The jet expands radially along the reactor height, what is noticeable by the black upward facing vectors. Due to the excess velocity of the jet, external air is suctioned inwards (white vectors), causing the so-called entrainment. This air of entrainment is responsible for the quenching of the system.

The ratio of entrainment ($E$), given by the ratio between the mass flow at a determined position and the initial mass flow ($E = \dot{m}/\dot{m}_0$) is also compared in Fig.2. Very similar profiles are observed for all the considered cases. The linear behavior is expected given the aspects of the process, being dependent on the nozzle characteristics, as well as fluid density, what also explains the similarity of the obtained profiles (Ricou and Spalding, 1961).

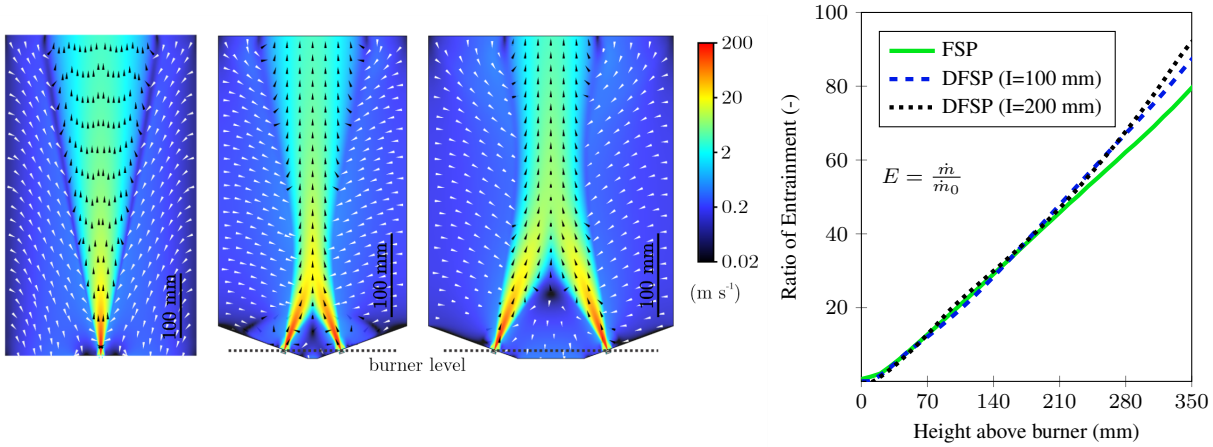


Figure 2. Velocity profiles overlaid with vectors for simulated cases (left), accompanied by the ratio of entrainment ($E$) along reactor height (right).

#### 3.1.2 Temperature

The thermal profiles play an important role in this process. Temperature has great influence over particle evolution, mainly regarding sintering, that is responsible for primary particle growth. Figure 3 shows both the temperature contours for the simulated cases and the profiles along center line and the flame axis (in the single-flamed case, these lines coincide). The highest temperatures are reached in the reaction zone, at about 50 mm of height. Similar values are observed for the profiles along the flame axis, what is expected given that the flames are under identical operation conditions. After the reaction zone is exited, the temperature drops rapidly with the increase of height due to the air of entrainment. In the DFSP cases, a small increase in temperature is observed at the position where the flames intersect.

Observing the profiles along the center line of the DFSP cases, it is noticeable that a larger portion of the domain is kept at lower temperatures, before the flames intersect. This, however, does not seem to significantly influence final particle size, as will be discussed in the next section.

### 3.2 Nanoparticles

With the converged flame sprays, the monodisperse PBM was solved. The PBM is written in terms of the surface area ($A$) and the volume ($V$) of the agglomerates of particles. These variables, however, are not ideal for the analysis of the final product. Better alternatives are the diameter of the primary particles ($d_{prim}$), and of the agglomerates ($d_{agg}$),defined as:

$$d_{prim} = \frac{6V}{A}, \text{and} \tag{10}$$

$$d_{agg} = \sqrt[3]{\frac{6V}{\pi}}. \tag{11}$$

Figure 3 shows the profiles of these variables along reactor height, which correspond to number weighted averaged values over planes parallel to the basis of the reactor. As it is noticeable for all he considered cases, the values of $d_{prim}$ and $d_{agg}$ coincide for the lower portions of the domain. That happens due to the high temperatures found in the region, that guarantees complete sintering of the agglomerates. After exiting the hot zone, neverhteless, there is not enough energy for sintering to happen, and the primary particles cease growing. Agglomeration, however, continues throughout the reactor, ever increasing agglomerate size. The height at which this happens is indicated in the plots by the dotted lines. Similar values are found for all cases, and the double flame with I = 100 mm result is closer to the ones of the single flame, what is in agreement with the observations from Grossmann *et al.* (2015), that show similar experimental behavior between these cases.

The final primary particle size, however, is estimated to be 6.3% smaller for the DFSP case with I = 100 mm, when

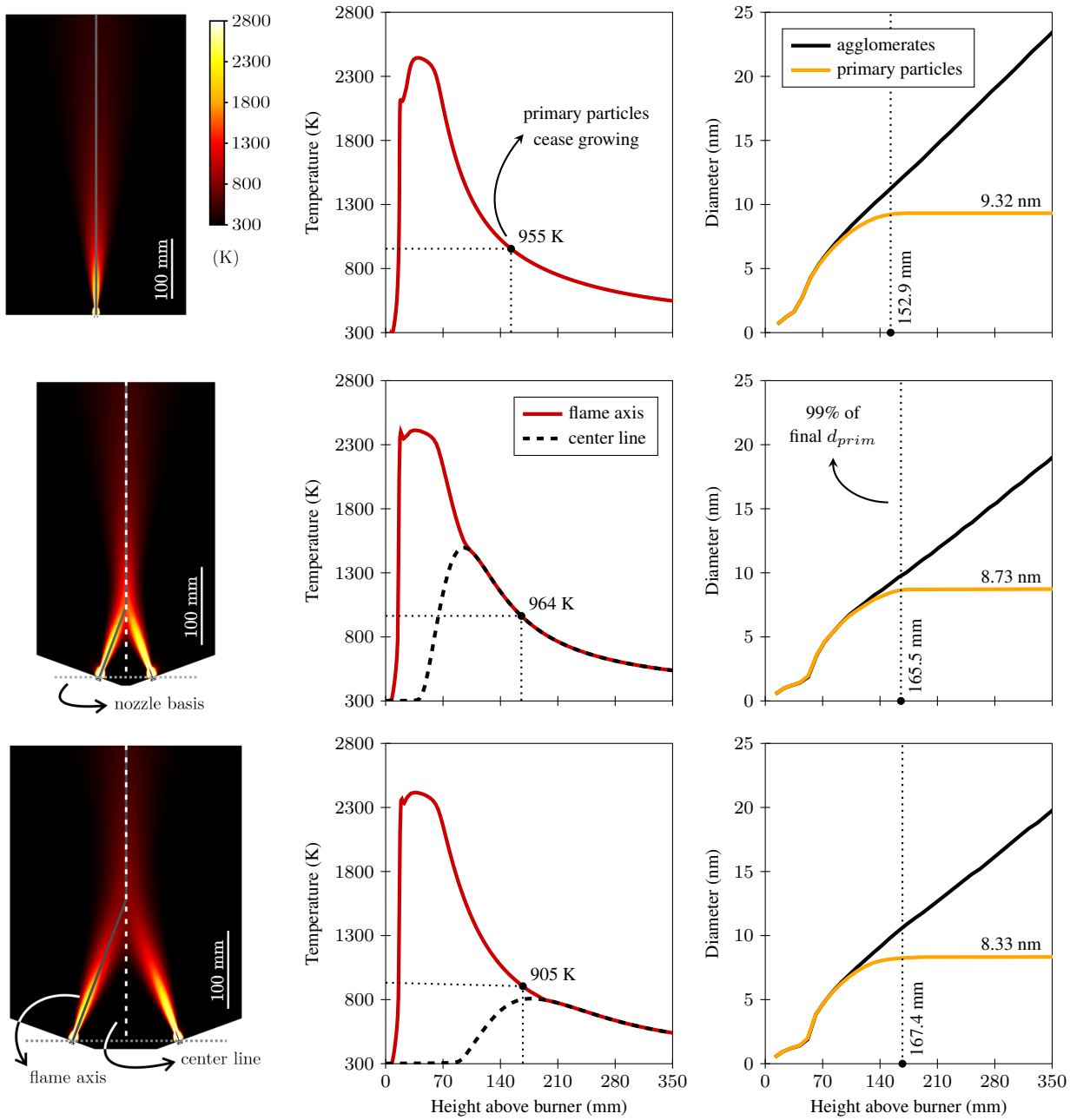


Figure 3. Flame temperature contours for simulated cases (left), accompanied by thermal profiles along center line and flame axis (center), and resultant diameters, both for primary particles and agglomerates, obtained for each case with the solution of the PBM (right).

compared to the case with the single flame. That should be result from the higher dilution present in the cases with two flames. Increase in the dilution of the nanoparticles cause a decrease in particle agglomeration inside the region with the highest temperatures, and, even though complete sintering is observed, agglomerates in that region are smaller, thus generating smaller primary particles. This assumption is supported with the comparison between the two DFSP cases. The case with I = 200 mm shows a decrease of 10.6% in the final size of the primary particles when compared to the case with the single flame (4.6%, when compared to the other DFSP case). A similar tendency is observed also outside the hot region, with the final size of agglomerates $\sim$10% bigger for the case with the single flame.

The similar results of primary particle and agglomerate sizes is due to the fact that $ZrO_2$ particles start to form close to the nozzle tip (Mueller *et al.*, 2004) and, by the time the flames meet, the particle formation is well advanced. This means that the particles have formed individually and at the time of mixing they only agglomerate and do not sinter into a single particle (Strobel *et al.*, 2006). Similar result was also observed by Grossmann *et al.* (2015), who showed that the size and crystallinity of the Ti particles are almost unaffected by double-flame configurations, whilst for the Pt particles (which start to form further downstream the flame) different results were obtained. Despite that, the final mix characteristics of multicompound materials can still be influenced and the double-flame configuration is still preferred for these applications, even when no significant change is observed in particle size (Strobel *et al.*, 2006).

## 4. CONCLUDING REMARKS

Computational Fluid Dynamics coupled with a monodisperse Population Balance Model (PBM) was applied to compare the velocity and temperature profiles, as well as primary particle and agglomerate mean diameters in Flame Spray Pyrolysis reactors of single flame and double flame reactors, with two different double flame configurations.

A similar entrainment behavior was observed in all cases, which is expected due to the analogous conditions. The flame axis temperature profiles are also very similar, but for the center axis in DFSP reactors the temperature decreases with the intersectional distance. Larger agglomerates were produced by the FSP process in comparison with the DFSP cases. The agglomerates and primary particle sizes were not significantly affected by the geometrical configurations of the two-nozzle setup, which could be related to the material system, which is closely related to the final particle characteristics. Therefore, the development of PBM capable of representing the agglomerates mass fraction is fundamental for accurate description of the multicompound nanoparticle synthesis.

Further investigation should involve the analysis of asymmetric reactors, and how the different configuration can affect flow patterns and final particle characteristics.

## 5. ACKNOWLEDGEMENTS

This study received funding from the German Research Foundation (DFG, Project ID: FR 912/33), Coordination for the Improvement of Higher Education Personnel (CAPES, Project ID: 20/2012) and São Paulo Research Foundation – FAPESP (Project ID: 2017/04045-0), in Brazil.

## 6. REFERENCES

Bamwenda, G.R., Tsubota, S., Nakamura, T. and Haruta, M., 1997. "The influence of the preparation methods on the catalytic activity of platinum and gold supported on TiO2 for CO oxidation". *Catalysis Letters*, Vol. 44, No. 1-2, pp. 83–87. ISSN 1011372X. doi:10.1023/a:1018925008633.

Bianchi Neto, P., Buss, L., Meierhofer, F., Meier, H.F., Fritsching, U. and Noriler, D., 2018. "Combustion kinetic analysis of flame spray pyrolysis process". *Chemical Engineering and Processing - Process Intensification*, Vol. 129, pp. 17–27.

Bianchi Neto, P., Meierhofer, F., Meier, H.F., Fritsching, U. and Noriler, D., 2020. "Modelling polydisperse nanoparticle size distributions as produced via flame spray pyrolysis". *Powder Technology*, Vol. 370, pp. 116–128. ISSN 1873328X. doi:10.1016/j.powtec.2020.05.019.

Buss, L., Meierhofer, F., Bianchi Neto, P., Meier, H.F., Fritsching, U. and Noriler, D., 2018. "Impact of co-flow on the spray flame behaviour applied to nanoparticle synthesis". *The Canadian Journal of Chemical Engineering*, Vol. 9999, No. 2, pp. 1–12. ISSN 1939019X. doi:10.1002/cjce.23386.

Buss, L., Noriler, D. and Fritsching, U., 2020. "Impact of Reaction Chamber Geometry on the Particle-Residence-Time in Flame Spray Process". *Flow, Turbulence and Combustion*. ISSN 15731987. doi:10.1007/s10494-020-00187-1. URL `https://doi.org/10.1007/s10494-020-00187-1`.

Celik, I., Ghia, U., Roache, P.J., Freitas, C.J., Coleman, H. and Raad, P.E., 2008. "Procedure for Estimation and Reporting of Uncertainty Due to Discretization in CFD Applications". *Journal of Fluids Engineering*, Vol. 130, No. 7, p. 078001. ISSN 00982202. doi:10.1115/1.2960953. URL `http://fluidsengineering.asmedigitalcollection.asme.org/article.aspx?articleid=1434171`.

Gröhn, A.J., Pratsinis, S.E. and Wegner, K., 2014. "Scale-up for nanoparticle synthesis by flame spray pyrolysis : the

high temperature particle residence time". *Industrial and Engineering Chemistry Research*, Vol. 53, pp. 10734–10742. doi:10.1021/ie501709s.

Grossmann, H.K., Grieb, T., Meierhofer, F., Hodapp, M.J., Noriler, D., Gröhn, A.J., Meier, H.F., Fritsching, U., Wegner, K. and Mädler, L., 2015. "Nanoscale mixing during double-flame spray synthesis of heterostructured nanoparticles". *Journal of Nanoparticle Research*, Vol. 17, pp. 1–16. ISSN 1388-0764. doi:10.1007/s11051-015-2975-8.

Li, W.C., Comotti, M. and Schüth, F., 2006. "Highly reproducible syntheses of active Au/TiO 2 catalysts for CO oxidation by deposition-precipitation or impregnation". *Journal of Catalysis*, Vol. 237, pp. 190–196. doi: 10.1016/j.jcat.2005.11.006. URL `www.elsevier.com/locate/jcat`.

Mädler, L., Kammler, H.K., Mueller, R. and Pratsinis, S.E., 2002. "Controlled synthesis of nanostructured particles by flame spray pyrolysis". *Journal of Aerosol Science*, Vol. 33, No. 2, pp. 369–389. ISSN 00218502. doi:10.1016/S0021-8502(01)00159-8. URL `http://www.sciencedirect.com/science/article/pii/S0021850201001598`.

Mehta, M., Raman, V. and Fox, R.O., 2013. "On the role of gas-phase and surface chemistry in the production of titania nanoparticles in turbulent flames". *Chemical Engineering Science*, Vol. 104, No. 2013, pp. 1003–1018. ISSN 00092509. doi:10.1016/j.ces.2013.10.039.

Meierhofer, F., Hodapp, M.J., Achelis, L., Buss, L., Noriler, D., Meier, H.F. and Fritsching, U., 2014. "Investigation of atomization concepts for large-scale flame spray pyrolysis (FSP)". *Materialwissenschaft und Werkstofftechnik*, Vol. 45, No. 8, pp. 765–778. ISSN 09335137. doi:10.1002/mawe.201400314.

Minnermann, M., Grossmann, H.K., Pokhrel, S., Thiel, K., Hagelin-Weaver, H., Bäumer, M. and Mädler, L., 2013. "Double flame spray pyrolysis as a novel technique to synthesize alumina-supported cobalt Fischer-Tropsch catalysts". *Catalysis Today*, Vol. 214, pp. 90–99. ISSN 09205861. doi:10.1016/j.cattod.2013.04.001.

Mueller, R., Jossen, R., Kammler, H.K., Pratsinis, S.E. and Akhtar, M.K., 2004. "Growth of zirconia particles made by flame spray pyrolysis". *AIChE Journal*, Vol. 50, No. 12, pp. 3085–3094. ISSN 00011541. doi:10.1002/aic.10272.

Noriler, D., Rosebrock, C.D., Mädler, L., Meier, H.F. and Fritsching, U., 2014a. "Influence of atomization and spray parameters on the flame spray process for nanoparticle production". *Atomization and Sprays*, Vol. 24, No. 6, pp. 495–524. ISSN 1044-5110. doi:10.1615/AtomizSpr.2014008559.

Noriler, D., Hodapp, M.J., Decker, R.K. and Meier, H.F., 2014b. "Numerical Simulation of Flame Spray Pyrolysis Process for nanoparticle productions: effects of 2D and 3D approaches". In *Proceedings of the ASME 2014*. pp. 1–9.

Ramkrishna, D., 2000. *Population balances*. Academic Press, San Diego, 1st edition. ISBN 0125769709. doi: 10.1016/B978-012576970-9/50007-2.

Ranz, W.E. and Marshall, W.R., 1952. "Evaporation from drops". *Chemical Engineering Progress*, Vol. 48, pp. 141–146.

Ricou, F.P. and Spalding, D.B., 1961. "Measurements of entrainment by axiisymmetrical turbulent jets". *Journal of Fluid Mechanics*, Vol. 11, pp. 21–32.

Strobel, R., Mädler, L., Piacentini, M., Maciejewski, M., Baiker, A. and Pratsinis, S.E., 2006. "Two-nozzle flame synthesis of Pt/Ba/Al2O3 for NO x storage". *Chemistry of Materials*, Vol. 18, No. 10, pp. 2532–2537. ISSN 08974756. doi: 10.1021/cm0600529. URL `https://pubs.acs.org/sharingguidelines`.

Teoh, W.Y., Amal, R. and Mädler, L., 2010. "Flame spray pyrolysis: an enabling technology for nanoparticles design and fabrication." *Nanoscale*, Vol. 2, No. 8, pp. 1324–1347. ISSN 2040-3364. doi:10.1039/c0nr00017e.

Torabmostaedi, H. and Zhang, T., 2014. "Numerical optimization of quenching efficiency and particle size control in flame synthesis of ZrO2 nanoparticles". *Journal of Thermal Spray Technology*, Vol. 23, No. 8, pp. 1478–1492. doi: 10.1007/s11666-014-0148-4.

Torabmostaedi, H., Zhang, T., Foot, P., Dembele, S. and Fernandez, C., 2013. "Process control for the synthesis of ZrO2 nanoparticles using FSP at high production rate". *Powder Technology*, Vol. 246, pp. 419–433. ISSN 00325910. doi:10.1016/j.powtec.2013.05.006. URL `http://linkinghub.elsevier.com/retrieve/pii/S0032591013003525`.

Wegner, K. and Pratsinis, S.E., 2005. "Gas-phase synthesis of nanoparticles: Scale-up and design of flame reactors". *Powder Technology*, Vol. 150, pp. 117–122. ISSN 00325910. doi:10.1016/j.powtec.2004.11.022.

## 7. RESPONSIBILITY NOTICE

The authors are the only responsible for the printed material included in this paper.